

6. Pyörälä K. Relationship of glucose tolerance and plasma insulin to the incidence of coronary heart disease: results from two population studies in Finland. *Diabetes Care* 1979;2:131-141.
7. Vaccaro O, Ruth KJ, Stamler J. Relationship of postload plasma glucose to mortality with 19-yr follow up. *Diabetes Care* 1992;15:1328-1334.
8. Phillips WT, Schwartz JG, McMahan CA. Rapid gastric emptying of an oral glucose solution in type 2 diabetic patients. *J Nucl Med* 1992;33:1496-1500.
9. Schwartz JG, McMahan CA, Green GM, Phillips WT. Gastric emptying in Mexican Americans compared to non-Hispanic whites. *Dig Dis Sci* 1995;40:624-630.
10. Horowitz M, Edelbroek MAL, Wishart JM, Straathof JW. Relationship between oral glucose tolerance and gastric emptying in normal healthy subjects. *Diabetologia* 1993;36:857-862.
11. American Diabetes Association. Clinical practice recommendations. *Diabetes Care* 1996;19(suppl1):S1-S18.
12. American Diabetes Association: Clinical Practice Recommendations. Office guide to diagnosis and classification of diabetes mellitus and other categories of glucose intolerance. *Diabetes Care* 1995;18:4.
13. Moore JG, Christian PE, Taylor AT, Alazraki N. Gastric emptying measurement: delayed and complex emptying patterns without appropriate correction. *J Nucl Med* 1985;26:1206-1210.
14. Hollander M, Wolfe D. *Nonparametric statistical methods*. New York: Wiley; 1973:27-33, 191-192.
15. Salomaa VV, Strandberg TE, Vanhanen H, et al. Glucose tolerance and blood pressure: Long term follow up in middle aged men. *BMJ* 1991;302:493-496.
16. Modan M, Halkin H, Almog S. Hyperinsulinemia: a link between hypertension, obesity and glucose intolerance. *J Clin Invest* 1985;75:809-817.
17. Florey CdV, Uppal S, Lowy C. Relation between blood pressure, weight and plasma sugar and serum insulin levels in school children aged 9-12 years in Westland, Holland. *BMJ* 1976;1:1368-1371.
18. Jarrett RJ, Keen H, McCartney M. Glucose tolerance and blood pressure in two population samples: their relation to diabetes mellitus and hypertension. *Int J Epidemiol* 1978;7:15-24.
19. Frank J, Saslow S, Camilleri M, et al. Mechanism of accelerated gastric emptying of liquids and hyperglycemia in patients with type II diabetes mellitus. *Gastroenterology* 1995;109:755-765.
20. Liddle RA, Rushokoff RJ, Morita ET, et al. Physiologic role for cholecystokinin in reducing postprandial hyperglycemia in humans. *J Clin Invest* 1988;81:1675-1681.
21. Phillips WT, Schwartz JG, McMahan CA. Reduced postprandial blood glucose levels in recently diagnosed noninsulin-dependent diabetics secondary to pharmacologically induced delayed gastric emptying. *Dig Dis Sci* 1993;38:51-58.
22. Schwartz JG, Guan D, Green GM, Phillips WT. Treatment with an oral proteinase inhibitor slows gastric emptying and acutely reduces glucose and insulin levels after a liquid meal in type II diabetic patients. *Diabetes Care* 1994;17:255-262.
23. Brener W, Hendrix TR, McHugh PR. Regulation of the gastric emptying of glucose. *Gastroenterology*. 1983;85:76-82.
24. Phillips WT, Schwartz JG, Blumhardt R, McMahan CA. Linear gastric emptying of hyperosmolar glucose solutions. *J Nucl Med* 1991;32:377-381.
25. Weytjens C, Keymeulen B, Segers O, et al. Rapid gastric emptying in noninsulin-dependent diabetes is not restricted to the early phase of disease [Abstract]. *Diabetologia* 1995;38:A32.
26. Nowak TV, Roza AM, Weisbruch JP, Brosnan MR. Accelerated gastric emptying in diabetic rodents: effect of insulin treatment and pancreas transplantation. *J Lab Clin Med* 1994;123:110-116.
27. Schwartz JG, Phillips WT, Guan D, Green GM. Gastric emptying of liquid meals is accelerated in the Zucker diabetic rat [Abstract]. *Diabetes* 1993;42:142.
28. Young AA, Gedulin B, Vine W, Percy A, Rink TJ. Gastric emptying is accelerated in diabetic BB rats and is slowed by subcutaneous injection of amylin. *Diabetologia* 1995;38:642-648.
29. Tosetti C, Corinaldesi R, Stanghellini V, et al. Gastric emptying of solids in morbid obesity. *Int J Obes* 1996;20:200-205.
30. Wisén O, Hellström PM. Gastrointestinal motility in obesity. *J Intern Med* 1995;237:411-418.
31. Horowitz M, Collins PJ, Cook DJ, Harding PE, Shearman DJC. Abnormalities of gastric emptying in obese patients. *Int J Obes* 1982;7:415-421.
32. Sasaki H, Nagulesparan M, Dubois A, et al. Hyperinsulinemia in obesity: lack of relation to gastric emptying of glucose solution or to plasma somatostatin levels. *Metabolism* 1983;32:701-705.
33. Hunt JN, Cash R, Newland P. Energy density of food, gastric emptying and obesity. *Am J Clin Nutr* 1978;31:S259-260.
34. Wright RA, Kim YC, Fleeman C. Solid and liquid gastric emptying in obese patients [Abstract]. *Gastroenterology* 1981;80:1320.
35. Horst GVD, Wesso I, Burger AP, Dietrich DLL, Grobler SR. Chemical analysis of cool drinks and pure fruit juices—some clinical implications. *S Afr Med J* 1984;66:755-758.
36. Schwartz JG, Phillips WT, Blumhardt MR, Langer O. Use of a more physiologic oral glucose solution during screening for gestational diabetes mellitus. *Am J Obstet Gynecol* 1994;171:685-691.

Photopenia in Chronic Vertebral Osteomyelitis with Technetium-99m-Antigranulocyte Antibody (BW 250/183)

Stefan Gratz, Hans-Gottfried Braun, Thomas M. Behr, Johannes Meller, Axel Herrmann, Monika Conrad, Doris Rathmann, Rudolf Bertagnoli, Hans-Georg Willert and Wolfgang Becker
 Departments of Nuclear Medicine and Orthopedics, Georg-August University of Göttingen, Germany

Photon-deficient areas in $^{99m}\text{Tc}/^{111}\text{In}$ white blood cell (WBC) images for diagnosing vertebral osteomyelitis have been published often. This study retrospectively evaluated whether the use of ^{99m}Tc -labeled monoclonal antigranulocyte antibodies (BW 250/183) is superior to WBC and whether it offers higher specificity. **Methods:** The study included 81 patients (46 men, 35 women; mean age 55 ± 2 yr; from 1989 to 1995) with clinically suspected vertebral osteomyelitis who underwent scintigraphic imaging after intravenous injection of 555 MBq ^{99m}Tc -labeled monoclonal antigranulocyte antibodies. Forty patients suffered from osteomyelitis (20 men, 20 women; mean age 56 ± 6 yr), 6 patients had metastases, 28 patients had spondylosis and disk herniation and 5 patients vertebral compression fractures. Diagnosis was not histologically verified in 2 patients. Planar imaging was performed at 4 and 24 hr postinjection. Histology of osteomyelitis was available in 30 patients, clinical follow-up in 10 patients. Visual uptake scores and quantita-

tive uptake scores of the suspected areas were calculated. The results were compared to a semiquantitative histological score (high, medium, low grade) as well as to the scintigraphic scores. **Results:** Scintigraphy showed photopenia in all patients with histologically proven vertebral osteomyelitis, independent of the grade of infection. A quantitative evaluation of 4 and 24 hr postinjection demonstrated a 58% increase of the uptake score in cases of histologically proven high-grade infections. This increase was seen predominantly in the thoracic spine but not in lumbar spine. All nonosseous paravertebral abscesses ($n = 2$) showed positive images and an increasing uptake over 24 hr. **Conclusion:** Paravertebral soft tissue infections can be differentiated excellently, whereas vertebral osteomyelitis, vertebral tumors or fractures can be localized, but no differentiation is possible.

Key Words: vertebral osteomyelitis; technetium-99m antigranulocyte antibodies; photopenic lesion; quantitative uptake

J Nucl Med 1997; 38:211-216

Received Feb. 28, 1996; revision accepted June 13, 1996.
 For correspondence or reprints contact: W. Becker, MD, Prof. of Nuclear Medicine, Department of Nuclear Medicine, University of Göttingen, Robert Koch-str. 40, D-37075 Göttingen, Germany.

Nuclear medicine imaging is able to provide information on changes in pathophysiological and pathobiochemical processes

in the patient, whereas morphologically based imaging provides information of the morphological changes in a specific process with high resolution. Nuclear medicine imaging is available as whole-body imaging in clinical routine, whereas CT, MRI and other techniques usually provide information on only part of the body.

Chronic vertebral osteomyelitis rarely initiates as a primary form of bone infection. In most of the cases, it is secondary to a short phase of acute bone infection. Acute osteomyelitis normally is due to a hematogenous penetration of the bacterias into the bone. At this time, clinical findings are slight and often confused with muscle tenseness. Without medical treatment, the acute phase of bone infection becomes chronic within a few weeks. In this phase of the bone infection, antibacterial chemotherapy can no longer be used.

For the localization and diagnosis of an infectious process, a nuclear medical procedure needs high sensitivity in all areas of the body. Additionally, after the localization of an infection, further investigation such as CT, MRI, biopsy and culture may be needed. For the differential diagnosis between infection, tumor, fracture or degenerative processes, a highly specific method is necessary.

Gallium-67 citrate and ^{111}In -labeled leukocytes have been described in the literature for the localization of suspected vertebral osteomyelitis (1). The results of white blood cell imaging were not satisfactory because photopenia was predominant (2-4). The cause may be very high pressure in a disk with chronic infection, so that proteins and granulocytes are prevented from migrating in the focus during the available time for imaging (2). Furthermore, few granulocytes can be detected histologically. Four of five patients with vertebral osteomyelitis were reported by Fernandez-Ulloa 1985 (5) to have shown a cold spot in the spine using ^{111}In white blood cells (WBC). One patient had a positive ^{111}In WBC scintigram. In this case *S. aureus* was isolated from the vertebral infectious process, which is known to produce soluble bacterial factors that are chemotactic to leukocytes. Thus, the bacteriologic characteristics of the infections may be another cause. Gallium-67 citrate may be superior to labeled leukocytes (1).

The advantages of $^{99\text{m}}\text{Tc}$ antigranulocyte antibodies over the autologous leukocyte technique in the imaging of infection are its simplicity of use, the lower radiation exposure to the patient, wide availability and excellent image quality due to an endogenous background subtraction (6). The antigranulocyte antibody is an IgG type that targets NCA-95 epitope on the surface of granulocytes. This study evaluated the diagnostic accuracy of $^{99\text{m}}\text{Tc}$ antigranulocyte antibodies in patients with chronic osteomyelitis of the spine.

METHODS

Patients

Eighty-one patients with clinically suspected vertebral osteomyelitis (46 men, 35 women; mean age 55 ± 2 yr), who were examined scintigraphically between 1989 and 1995 with 555 MBq $^{99\text{m}}\text{Tc}$ -labeled monoclonal antigranulocyte antibodies, were examined retrospectively. Of these patients, 40 (20 men, 20 women; mean age 56 ± 6 yr) suffered from osteomyelitis of the spine, 6 patients showed metastases, 28 patients spondylosis and disk herniation and 5 patients had vertebral compression fractures. No diagnosis was established in 2 patients. All 81 patients were examined with the $^{99\text{m}}\text{Tc}$ -labeled antigranulocyte antibody BW 250/183 (Behring-Werke, Marburg, Germany). Postoperative histology was available in 53 patients. In 30 patients, vertebral osteomyelitis was biopsy-proven, and in 10 patients final diagnosis

of vertebral osteomyelitis was evaluated by clinical follow-up and response to medical treatment. In all 81 patients radiological results were compared with scintigraphy. Five of the 30 patients with biopsy-proven vertebral osteomyelitis had more than one infected focus in the vertebral spine. Thus, a total of 40 spinal regions were located: in the thoracic (Th) spine ($n = 13$; TH 7/8 = 4, TH 10/11 = 3, TH 11/12 = 6), lumbar (L) and sacral (S) spine ($n = 27$; TH 12/L 1 = 4, L1/2 = 4, L 2/3 = 6, L 4/5 and S 1 = 13).

Further bioptical findings were metastases in two patients, spondylosis and disk herniation in 21 patients, whereas the final diagnosis of the remaining patients was done by CT and MRI.

Antibody Characterization

The $^{99\text{m}}\text{Tc}$ -labeled antibody (BW 250/183) is an IgG1 isotype and detects a 95-kDalton glycoprotein. The epitope recognized is localized on CEA and NCA-95. The epitope is expressed on the surface of granulocytes, promyelocytes and myelocytes, which are targeted by the antibody. The affinity constant of the $^{99\text{m}}\text{Tc}$ antigranulocyte antibody was determined to be $2 \times 10^9 M$ (6).

BW 250/183 does not influence granulocyte mediated functions (6). Approximately 10%-20% of the radiolabeled injected antibody is bound to circulating granulocytes that are functionally normal and may target an infectious area. Approximately 19% of the injected antibody circulates as free immunoglobulin and has probably the same targeting potential as labeled nonspecific human IgG (7).

Imaging

Antigranulocyte antibody imaging was performed at 4 and 24 hr after injection of 555 MBq $^{99\text{m}}\text{Tc}$ -labeled antigranulocyte antibody. Imaging was performed with a double-headed large field-of-view gamma camera (Prism 2000) on line with an Odyssey 1500 computer system, equipped with a low-energy high-resolution collimator. We used 20% windows, centered over the 140-keV photopeak of $^{99\text{m}}\text{Tc}$. In all cases, whole-body images were performed in anterior and posterior projection over 15 min. Quantitative uptake measurements were performed in the vertebral ROI at 4 and 24 hr postinjection to evaluate an increase or decrease over the time. With the ROI technique, suspected vertebral bodies were quantitatively evaluated using count ratios between affected and nonaffected vertebrae.

Image Interpretation

Radiotracer uptake of a diseased vertebral body in antigranulocyte antibody images was measured quantitatively (Picker Prism 2000, acquisition matrix 256×256). For this purpose, ROIs over two suspected adjacent vertebral bodies were compared with identically sized ROIs over two normal vertebral bodies. The results were correlated with histological findings and with the localization in the spine. The count rates were classified as normal (equal to adjacent bone marrow), increased or decreased. For analysis, three different criteria for description were defined: (a) increasing activity from 4 hr to 24 hr; (b) decreasing activity from 4 hr to 24 hr; and (c) no change of activity over time.

In conventional radiology, typical findings for infection of adjacent vertebrae were considered: the diminution of the intervertebral disk and subchondral sclerosis in cases of low disease activity. Most of the cases showed reduction in mineral salt and reduced thickness of the adjacent upper and lower end plate.

Histologic specimens were classified as:

1. High-grade, specific ($n = 3$) with caseation or not, productive or exudative, presence of epitheloid cell wall, plasma cells and lymphocytic infiltrate.
2. High-grade, nonspecific ($n = 13$) with mucous, necrotic-granular, plasma cells, lymphocytic infiltrate ($n = 5$) plasma cells and lymphocytes only ($n = 8$).

3. Medium-grade, nonspecific (n = 12) with plasma cells, lymphoplasma-cellular infiltrates, beginning granulation and scar tissue.
4. Low-grade, nonspecific (n = 2) with very little lymphoplasmacellular infiltrate, mostly sclerosis and scar tissue.

Statistical Analysis

Mean values, s.d. and significance of the uptake measurements from 4 to 24 hr were evaluated. The paired chi-square test was used to compare paired values.

RESULTS

Eighty-one patients with suspected vertebral osteomyelitis underwent clinical examination and immunoscintigraphy. All lesions showed cold defects except infections outside bone. Forty cases of vertebral osteomyelitis were identified; 30 were confirmed by biopsy. In all 40 cases, clinical follow-up and radiological changes were consistent with osteomyelitis. Ten cases were stated as vertebral osteomyelitis by positive blood culture, radiological findings and clinical signs such as fever, leukocytosis and improvement after appropriate antibiotic therapy. In contrast to Palestro et al. (9), all patients with vertebral osteomyelitis showed decreased activity on antigranulocyte images independent of the grade of infection and duration of symptoms. The median duration of symptoms in patients with vertebral osteomyelitis varied between 1 wk and 3 mo. A correlation between median duration of symptoms and decreased activity could not be established. Final diagnosis in the remaining 41 cases were: 6 metastases, 28 spondylosis and disk herniations and 5 compression fractures. No diagnosis was established in 2 patients. Two patients with vertebral osteomyelitis had additional extra-osseous sites of paravertebral infection of the psoas muscle.

Histology showed, in cases of medium/low-grade osteomyelitis, very low content of granulocytes and the beginning of granulation/necrotic tissue. This could not be differentiated histologically from the activated form of vertebral arthritis. A differentiation between medium/low-grade osteomyelitis and vertebral arthritis was also not possible in the immunoscintigraphy (Figs. 1, 2). Metastases (breast and prostatic carcinomas) imposed with a sharp cut-off configuration of the vertebral bodies themselves, whereas in patients with vertebral arthritis the morphological configuration of two adjacent vertebral bodies showed a homogenous linear decreased uptake with predominantly marginal imposing photopenia.

Biopsy-proven tuberculous spondylitis showed an increase of the target/nontarget ratio (t/nt; mean 0.59/0.72) in one patient (productive, exsudative) and a decrease of the t/nt ratio (mean $0.61 \pm 0.01/0.41 \pm 0.01$, $p > 0.05$) in two patients (caseation, epitheloid). High-grade nonspecific osteomyelitis showed an increase of t/nt ratio (mean $0.75 \pm 0.04/0.84 \pm 0.06$, $p < 0.05$) in six patients, no increase of t/nt ratio (mean 0.74 ± 0.01 , $p > 0.05$) in eight patients and a decrease of t/nt ratio (mean $0.72 \pm 0.01/0.54 \pm 0.01$, $p > 0.05$) in two patients (lympho-plasmacellular). Medium-grade nonspecific osteomyelitis showed no increase of t/nt ratio (mean 0.63 ± 0.01 , $p > 0.05$) in four patients and a decrease of t/nt ratio (mean $0.65 \pm 0.01/0.49 \pm 0.01$, $p < 0.01$) in eight patients. Degenerative alterations showed no increase of t/nt ratio in one patient (0.71). The difference between the 4- to 24-hr t/nt ratio is statistically significant at $p < 0.05$ and $p < 0.01$, whereas at $p > 0.05$, there is no statistical significance.

Increasing uptake was evaluable only in thoracic or thoracic/lumbar vertebrae, whereas no increase was found in lumbar or sacral vertebrae. The nonspecific osteomyelitis of the thoracic

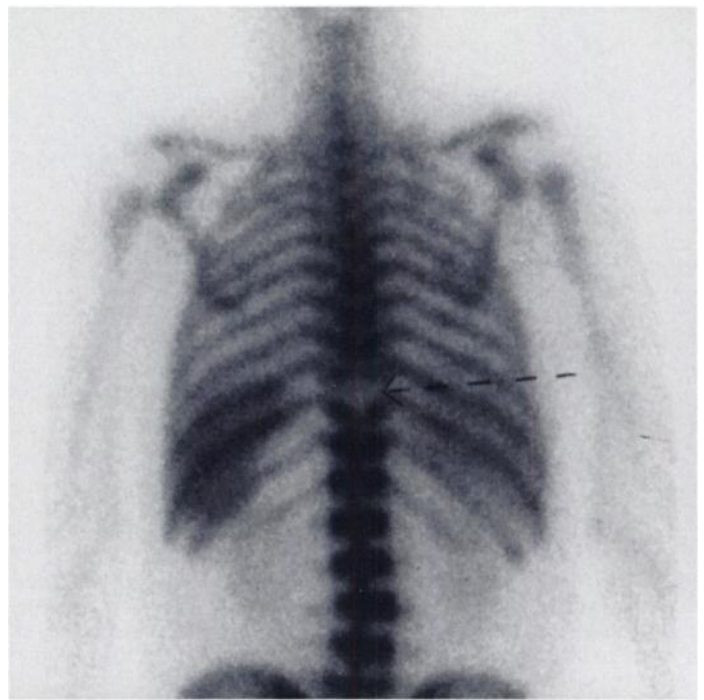


FIGURE 1. Decreased antibody uptake with a biconcave configuration over the two adjacent vertebral bodies in TH 9/10 in a 57-yr-old man with vertebral osteomyelitis and an increasing uptake from 4 to 24 hr postinjection. Histology: high grade, chronic bacterial osteomyelitis with necrotic tissue and high-grade septic granulocytic infiltration of intervertebral disk. No morphological differentiation was possible between tuberculous and bacterial osteomyelitis.

vertebrae was histologically classified as high grade, and a relative increase of 58.8% was measured. The results of visual uptake scores (n = 12, thoracic spine = 4, thoracic/lumbar spine = 3, lumbar spine = 5) were identical to the quantitative computerized measurements. Paravertebral abscesses always showed positive contrast and the uptake increase of the t/nt ratio was 25% and 30% (Fig. 3).

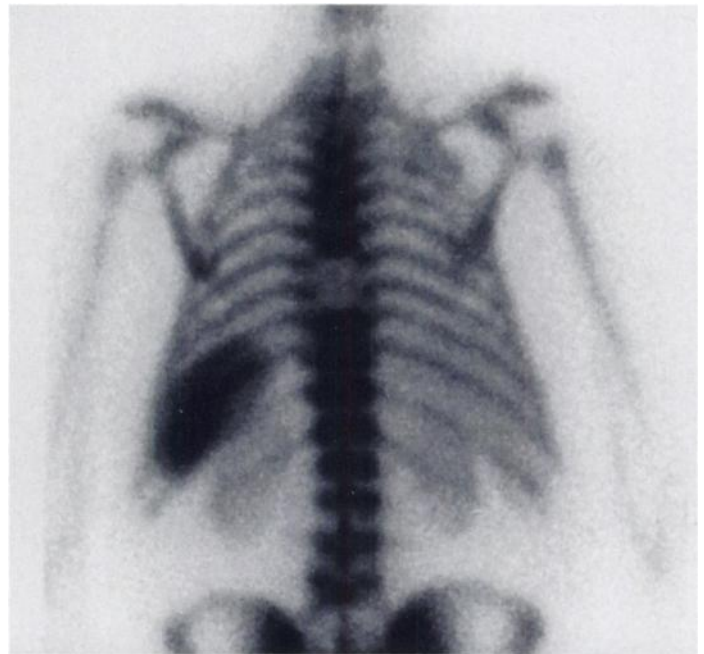


FIGURE 2. A 68-yr-old man with multifocal bone marrow infiltration of plasmocytoma. TH 7/8 and L 5 show decreased uptake with a sharp cutoff configuration. Initial clinical signs of vertebral osteomyelitis with lower back pain, intermediate fever and little leukocytosis. Conventional radiological findings were not conclusive.



FIGURE 3. A 63-yr-old woman with typical clinical signs of chronic vertebral osteomyelitis. Radiological findings of the suspected vertebrae were negative, immunoscintigraphy was positive in the right psoas muscle with increase over time. Additional positive uptake is in an abscess of the lower part of the left gluteal muscle. Histology of both sites: psoas abscess and abscess of gluteal muscle with pus, necrotic soft tissue and infiltration of granulocytes, plasma cells and lymphocytes.

Antigranulocyte antibody (BW 250/183) scintigraphy demonstrated high imaging quality. It was possible to establish a morphologically oriented description of the suspected vertebral bodies. Decreased activity was present in all 40 cases of vertebral osteomyelitis. Histological high-grade osteomyelitis was established with a decreased biconcave configured uptake over two adjacent vertebral bodies in all patients. No differentiation between nonspecific and specific (tuberculosis) osteomyelitis was possible (Fig. 4). Semiquantitative uptake ratio and histological results are compared in Table 1.



FIGURE 4. A 62-yr-old man with linear decreased activity with marginal photopenia. Histology: arthrosis with no signs of any grade of infection.

DISCUSSION

Patients with back pain are often seen clinically. A fast and correct diagnosis is necessary for immediate therapy. Often, differential diagnosis is difficult because the symptoms of chronic vertebral osteomyelitis, metastases and degenerative disease of the spine are identical. CT and MRI are known to have a high sensitivity and specificity in the differentiation of circumscribed lesions of the vertebral spine. High costs, high radiation exposure by CT and the low availability of the MRI limit the use of these two methods. Bone scans and immunoscintigraphy offer whole-body exposure with low radiation, high sensitivity and low cost. Although the extent of bone disease can be evaluated effectively, both methods show low specificity. Photon-deficient areas in bone scans have received a great deal of interest since their description (2). These cases were due to metastatic tumors, bone infarction or fractures. Other causes have been described, including radiation, osteomyelitis, metal artifacts and other rarer causes.

Mok et al. (2) in 1984 and Georgi et al. (8) in 1985 described skeletal photopenic lesions in whole-body scintigraphy independently from each other, using ^{111}In -labeled white blood cell imaging. In 1991, Palestro et al. (9) observed 76 ^{111}In -labeled leukocyte images performed on 71 patients with possible vertebral osteomyelitis, whereas in 38 patients a decreased vertebral activity was observed. Reuland et al. (10) used $^{99\text{m}}\text{Tc}$ -labeled murine Mabs directed against epitopes expressed on the surface of granulocytes in their prospective study of 106 orthopedic patients in early postoperative stages. They reported false-negative findings in the hips and spine, although positive findings in peripheral sites were dominant.

All results reported on white blood cell imaging were not satisfactory (9). Immunoscintigraphy and scintigraphy with $^{99\text{m}}\text{Tc}$ -HIG imaging is reported to show the same results (11).

Different pathophysiological processes have been discussed to explain cold defects. It may be that high pressure in one disk with chronic infection prevents proteins and granulocytes from migrating in the focus during the imaging time available. Another reason may be that the cold behavior is only relative, due to the normal bone marrow in the neighboring vertebral bodies. The epitope for the antigranulocyte antibody is expressed on the surface of granulocytes, promyelocytes and myelocytes. Approximately 10%–20% of the radiolabeled injected antibody is bound to circulating normal granulocytes. Approximately 19% of the injected antibody circulates as free immunoglobulin (12).

Another reason for photopenic lesions in vertebral osteomyelitis may be the low infiltration of granulocytes. In clinical routine in patients with nonspecific bacterial vertebral osteomyelitis, scintigraphy is often performed between 2 to 3 mo after onset of the first clinical symptoms, whereas in patients with tuberculous spondylitis, even longer periods are usual before the final diagnosis is established. Chronic osteomyelitis initiates in more than 50% as an original chronic type of osteomyelitis, which is resistant to antibiotics. In less than half of all patients with chronic vertebral osteomyelitis, it originates from an acute hematologic form, which responds to antibiotics, as long as it is active. Histological high-grade chronic osteomyelitis with a high content of granulocytes turns into medium- and low-grade chronic osteomyelitis after a few weeks (13). Normally low turnover of granulocytes is discussed in these patients. They probably represent the beginnings of a chronic stage with only little polymorphonuclear infiltration. Bacteriological characteristics (5) do not seem to be a reason for photopenia. In our findings, there were three patients with *S. aureus* infections. In two of them, high-grade vertebral osteo-

TABLE 1
Comparison of Semiquantitative Uptake Ratio to Histological Results

Histology	Patients (n)	4 hr postinjection t/nt ratio	24 hr postinjection t/nt ratio	Significance
Tuberculous osteomyelitis				
Productive, exsudative	1	0.59	0.72	
Caseation, epitheloid	2	0.61 ± 0.01	0.41 ± 0.01	p > 0.05
Bacterial osteomyelitis				
High-grade				
Increase	6	0.75 ± 0.04	0.84 ± 0.06	p < 0.05
No increase	8	0.74 ± 0.11	0.74 ± 0.10	p > 0.05
Decrease	2	0.72 ± 0.01	0.54 ± 0.01	p > 0.05
Medium-grade				
Increase	—	—	—	
No increase	4	0.63 ± 0.01	0.63 ± 0.01	p > 0.05
Decrease	8	0.65 ± 0.10	0.49 ± 0.12	p < 0.01
Degenerative disease				
No increase	1	0.71	0.71	

myelitis was biopsy-proven, and immunoscintigraphy of the spine showed a cold spot in this area. One patient had an abscess of the psoas and gluteal muscle, and both foci had positive contrast. Another possibility for photopenic lesions may be explained by Palestro (9) and Jacobson (14). Minor blood supply and blood circulation may be due to microthrombosis of the afferent blood vessels or due to fibrosis of the bone marrow. Vertebral osteomyelitis presumably starts as a septic embolism, located in the metaphyseal artery and endarteriole in the metaphysis of the vertebral bodies. This embolus propagates retrograde into the metaphyseal anastomosis, and circumferentially around the vertebral body, sequentially occluding other metaphyseal arteries. The regions of the vertebral metaphysis supplied by each of these metaphyseal arteries undergo sequential septic infarction producing osteomyelitis (9). High pressure on the vertebral disk seems to be highly favorable. This would explain why in our findings a relative semiquantitative increase of uptake could be estimated just in thoracic or thoraco/lumbar vertebrae and not in lumbar or sacral vertebrae, where natural pressure due to bodyweight is highest.

Morphologically decreased biconcave-configured uptake over two adjacent vertebral bodies, which was established in all patients with histologically proven high-grade vertebral osteomyelitis, seems to be due to the way vertebral osteomyelitis spreads. Vertebral osteomyelitis is mostly secondary to spondylodiscitis, and the infectious infiltration originates from the disk with consequent infiltration in the adjacent vertebral upper and lower end plate followed by consecutive septic infarction. In the absence of infection, granulocytes generally are not incorporated into areas of increased bone mineral turnover such as metastatic tumors and degenerative disorders.

Palestro et al. (9) reported a specificity of leukocyte imaging of 98%, when only increased activity was considered positive, compared with 71% for two-phase bone scintigraphy and 49% for delayed bone imaging. The sensitivity of this criteria was reported only to be 39% because more than half of their patients (54%) with vertebral osteomyelitis presented photopenia. Including decreased activity as a criterion for a positive study, the specificity was only 50%.

Our results show photopenia in all patients with proven vertebral osteomyelitis. If only increased activity is considered positive, the sensitivity and specificity of immunoscintigraphy in the spine has disappointing sensitivity and specificity. In comparison, the sensitivity for the detection of a spine pathology was 100%. However, a specific differentiation between

infection, metastasis and other pathologies is not possible. Also, the semiquantitative uptake measurement from 4 to 24 hr is not helpful because it is not uniform in the different pathologic grades of infection and allows no further differentiation to metastasis or degenerative alterations.

Our results indicate that BW 250/183 shows all vertebral osteomyelitic lesions as cold spots and that it is not a suitable agent for a specific detection of inflammatory diseases of the spine, whereas the sensitivity to detect a lesion is high. Abscesses of the soft tissue always show positive uptake. Although BW 250/183 is a ^{99m}Tc-labeled antigranulocyte antibody that is simple to use, readily available and of high imaging quality, there is no clinical advantage of immunoscintigraphy over ^{99m}Tc/¹¹¹In white blood cell imaging for the detection of osteomyelitis of the spine.

The antigranulocyte antibody (BW 250/183) has a large molecular size of 150 kDalton. Smaller fragments may have better capillary permeability and a more rapid whole-body clearance that may offer better target/background ratios at 4 to 6 hr postinjection (15).

Due to the smaller mole weight of 50 kDalton (16), better targeting of osteomyelitis of the spine may be expected. Thus, further examination with ^{99m}Tc antigranulocytes Fab'-fragments (15) are of interest to study the targeting behavior of osteomyelitis of the spine.

REFERENCES

- Elgazzar AH, Abdel-Dayem HM, Clark JD, Maxon HR. Multimodality imaging of osteomyelitis. *Eur J Nucl Med* 1995;22:1043-1063.
- Mok YP, Carney WH, Fernandez-Ulloa M. Skeletal photopenic lesions in ¹¹¹In WBC imaging. *J Nucl Med* 1984;25:1322-1326.
- Hotze AL, Briele B, Overbeck B, et al. Technetium-99m-labeled antigranulocyte antibodies in suspected bone infections. *J Nucl Med* 1992;33:526-531.
- Datz FL, Thorne DA. Cause, significance of cold bone defects on indium-111-labeled leukocyte imaging. *J Nucl Med* 1987;28:820-823.
- Fernandez-Ulloa M, Vasavada PJ, Hanslits ML, Volarich DT, Elgazzar AH. Diagnosis of vertebral osteomyelitis: clinical, radiological and scintigraphic features. *Orthopedics* 1985;8:1144-1150.
- Becker W, Borst U, Fischbach W, Pasurka B, Schäfer R, Börner W. Kinetic data of in vivo labeled granulocytes in humans with murine ^{99m}Tc-labeled monoclonal antibody. *Eur J Nucl Med* 1989;15:361-366.
- Becker W. The contribution of nuclear medicine to the patient with infection. *Eur J Nucl Med* 1995;22:1195-1211.
- Georgi P, Kaps HP, Sinn HJ. Leukozytenszintigraphie bei entzündlichen prozessen der wirbelsäule. *Radiologe* 1985;25:324-328.
- Palestro CJ, Kim DK, Swyer AJ, Vallabhajosula S, Goldsmith S. Radionuclide diagnosis of vertebral osteomyelitis: In-111-leukocyte and Tc-99m methylene diphosphonate bone scintigraphy. *J Nucl Med* 1991;32:1861-1865.
- Reuland P, Winker KH, Heuchert T, et al. Detection of infection in postoperative orthopedic patients with technetium-99m-labeled monoclonal antibodies against granulocytes. *J Nucl Med* 1991;32:2209-2214.
- Sciuc J, Brandau W, Vollet B, et al. Comparison of technetium-99m polyclonal human

- immunoglobulin and technetium-99m monoclonal antibodies for imaging chronic osteomyelitis. *Eur J Nucl Med* 1991;18:401-407.
12. Bosslet K, Lüben G, Schwarz A, et al. Immunohistochemical localization and molecular characteristics of three monoclonal antibody-defined epitopes detectable on carcinoembryonic antigen (CEA). *Int J Cancer* 1985;33:643.
13. Otte P, Schlegel KF. Aktuelle orthopädie, Behandlung der sekundär-chronischen osteomyelitis. Stuttgart, Germany: Ferdinand Enke Verlag; 1872;1-18.
14. Jacobson AF, Gilles CP, Cerqueira MD. Photopenic defects in marrow-containing skeleton on indium-111 leukocyte scintigraphy: prevalence at sites suspected of osteomyelitis and as an incidental finding. *Eur J Nucl Med* 1992;19:858-864.
15. Becker W, Bair J, Behr T, et al. Detection of soft-tissue infections and osteomyelitis using a technetium-99m-labeled antigranulocyte monoclonal antibody fragment. *J Nucl Med* 1994;35:1436-1443.
16. Serafini AN. From monoclonal antibodies to peptides and molecular recognition units: an overview. *J Nucl Med* 1993;34:533-536.

Changes in Results of Gallium-67-Citrate Scanning after Interferon Therapy for Chronic Hepatitis C

Susumu Shiomi, Tetsuo Kuroki, Tadashi Yokogawa, Tadashi Takeda, Shuhei Nishiguchi, Shinya Nakajima, Takashi Tanaka, Terue Okamura and Hironobu Ochi

Third Department of Internal Medicine, Department of Public Health and Division of Nuclear Medicine, Osaka City University Medical School, Osaka, Japan

Gallium-67 scanning is useful for early diagnosis and grading of interstitial lung disease. In a study of the side effects of interferon (IFN) on the lungs of patients with chronic hepatitis C, we performed ^{67}Ga scanning before and after IFN therapy. **Methods:** The 66 subjects who underwent at least one scanning, before IFN therapy, were 8 patients with chronic persistent hepatitis (CPH), 21 with chronic aggressive hepatitis 2A (CAH-2A), 25 with chronic aggressive hepatitis 2B (CAH-2B) and 12 with cirrhosis. All had underlying hepatitis C viral infection. Of those patients, 20 were examined again within 1 mo after IFN therapy. Patients received an intravenous injection of 340 MBq ^{67}Ga -citrate and were imaged 72 hr later. ROIs were established for anterior views of the lungs (Lu), liver (Li) and soft tissue of the upper arm as background (B). The counts per unit size of each region of interest were used in calculation of the ratios Lu/B and Li/B. **Results:** The medians of Lu/B were 2.46 in CPH, 2.56 in CAH-2A, 2.50 in CAH-2B and 2.47 in cirrhosis. These differences were not statistically significant. The medians of Li/B were 6.42 in CPH, 6.14 in CAH-2A, 5.11 in CAH-2B and 4.03 in cirrhosis. The differences between the median Li/B of cirrhotic patients and the medians for patients with CPH, CAH-2A and CAH-2B were significant. After therapy, Lu/B was higher than before in 16 of the 20 patients and lower in the four other patients; the overall rise was significant (Wilcoxon rank-sum test). Li/B was higher than before in 11 of the 20 patients and lower in the nine other patients. **Conclusion:** IFN caused uptake of the radionuclide to increase in most patients. This method showed changes in the accumulation of ^{67}Ga -citrate that could have been missed if the results had been inspected by eye. IFN can cause interstitial lung disease, but unlike other drugs with this side effect, the onset seems to be gradual enough to be detected quantitatively by ^{67}Ga scanning.

Key Words: gallium-67-citrate; interferon-alpha; hepatitis C; interstitial lung disease

J Nucl Med 1997; 38:216-219

Chronic hepatitis B is often treated with interferon (IFN) (1), which can cause such side effects as fever of 38°C or more, influenza-like symptoms, thrombocytopenia, leukocytopenia, proteinuria and alopecia (2). Administration is long term when infection is with the hepatitis C virus (3), and further side effects may appear. The most troublesome are autoimmune thyroid disease (4-6), autoimmune hepatitis (7,8), worsening

of diabetes mellitus (9,10), psychiatric disorders (11,12) and interstitial lung disease (13-17). Interstitial lung disease, in particular, has a poor prognosis, and early diagnosis and treatment are needed. Gallium-67 scanning is generally useful for the early diagnosis of interstitial lung disease (18). It might be improved by being made quantitative rather than qualitative. To identify the effect of IFN on the lungs, we performed ^{67}Ga scanning in patients with chronic hepatitis C before and after IFN therapy, with quantitative results used to monitor responses and, in some cases, to exclude patients from IFN therapy when uptake in the first scanning was unusually high.

MATERIALS AND METHODS

Patients

Sixty-six patients with underlying hepatitis C viral infection underwent at least one scanning (before IFN therapy). Thirty-six patients were men and 30 were women; the mean age was 50 yr (range 21-67 yr). Chronic hepatitis C was diagnosed by the detection of antibodies to hepatitis C virus. Diagnoses of the liver condition were based on histological examination of liver specimens obtained by laparoscopy or needle biopsy done under ultrasonic guidance between April 1993 and August 1995. Results of the histological examination, which was done by internationally established criteria (19), showed that there were eight patients with chronic persistent hepatitis (CPH), 21 patients with chronic aggressive hepatitis 2A (CAH-2A) with moderate piecemeal necrosis and inflammation (20), 25 patients with chronic aggressive hepatitis 2B in which these two signs were severe (CAH-2B) and 12 patients with cirrhosis of the liver. The ^{67}Ga scanning before therapy was done within 1 wk of liver biopsy. All patients were asked and 20 patients agreed to return as outpatients to be examined a second time within 1 mo of the end of IFN therapy. We classified all patients into three categories according to their changes in alanine aminotransferase (ALT) activity with IFN therapy. Responders were those in whom ALT activity at the end of IFN therapy was normal. Partial responders were those in whom ALT activity had decreased but not to the normal level by the end of IFN therapy. Nonresponders were those in whom ALT activity had not decreased by the end of IFN therapy. The clinical background of patients scanned twice and their responses to IFN therapy are shown in Table 1.

Received Jan. 9, 1996; revision accepted June 15, 1996.

For correspondence or reprints contact: Susumu Shiomi, MD, Third Department of Internal Medicine, Osaka City University Medical School, 1-5-7 Asahimachi, Abeno-ku, Osaka 545, Japan.